

Graphical Method for Kinetics of Polymerization. 4. Living Polymerization Initiated by Trifunctional Initiator with Nonequal Initiation Rate Constants

Deyue Yan

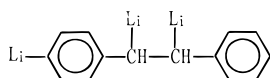
Department of Applied Chemistry, Shanghai Jiao Tong University, 1954 Hua Shan Road, Shanghai 200030, People's Republic of China

Received July 22, 1997; Revised Manuscript Received November 7, 1997

ABSTRACT: This work dealt with the kinetics of living polymerization initiated by a trifunctional initiator with nonequal initiation rate constants by way of the Laplace transformation and graphical method. The expressions of the molecular weight distribution function, the number- and the weight-average degrees of polymerization, and the distribution of branching were derived rigorously. The numerical results show that the influence of nonequal initiation rate constants on the molecular parameters of the resulting polymer is important at low monomer conversion and becomes negligible at high polymer yield.

Introduction

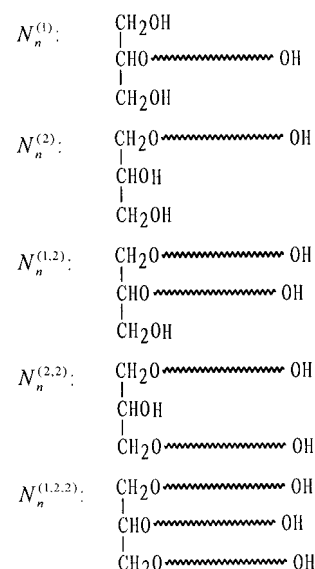
One of the primary methods for the synthesis of a star-shaped polymer is living polymerization with a multifunctional initiator.^{1,2} The author of this paper and co-workers^{3,4} have reported a kinetic theory for multifunctional living polymerization with equal initiation rate constant. Sometimes, the functional groups in a multifunctional initiator have nonequal reactivities. For instance, Kaspar and Trekoval⁵ claimed that the trifunctional organolithium compound,



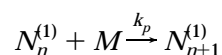
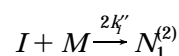
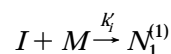
is useful for anionic polymerizations of diene and styrene, in which the active sites evidently possess different initiation rate constants. In addition, if glycerin is used as the initiator in the cationic polymerization of propylene oxide catalyzed by boron fluoride, the reactivity of the *sec*-hydroxy is different from that of *n*-hydroxy.⁶ In both examples mentioned, there is only one of the functional groups in the trifunctional initiator that is distinct from others in initiation rate constant. According to the reaction scheme given in the examples, a kinetic model is developed below, and the molecular weight distribution function and other molecular parameters of the resultant polymer are derived rigorously by way of Laplace transformation and the graphical method.^{3,7–9}

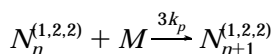
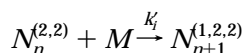
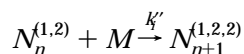
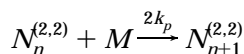
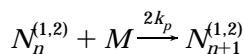
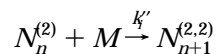
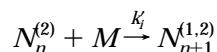
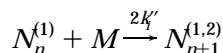
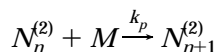
Kinetic Differential Equations

For instance, Shulga and Lebedev⁶ reported that in the cationic living polymerization system of propylene oxide initiated by glycerin, there are various species with different numbers of arms as shown below:



where $N_n^{(1)}$ and $N_n^{(2)}$ denote the concentrations of the one-arm species with n monomeric units generated respectively from different active sites of the trifunctional initiator; similarly, $N_n^{(1,2)}$ and $N_n^{(2,2)}$ represent the respective concentrations of the different two-arm species with n monomeric units; $N_n^{(1,2,2)}$ symbolizes the concentration of the three-arm n -mers; I and M are the concentrations of the initiator and the monomer, respectively. The reaction mechanism of the polymerization under consideration includes the following steps:





The set of kinetic differential equations appropriate to the polymerization system reads

$$dI/dt = -(k_i + 2k_i')IM \quad (1)$$

$$dN_1^{(1)}/dt = k_i'IM - k_pN_1^{(1)}M - 2k_i''N_1^{(1)}M \quad (2)$$

$$dN_n^{(1)}/dt = k_pN_{n-1}^{(1)}M - k_pN_n^{(1)}M - 2k_i''N_n^{(1)}M \quad (3)$$

$$dN_1^{(2)}/dt = 2k_i''IM - k_pN_1^{(2)}M - (k_i' + k_i'')N_1^{(2)}M \quad (4)$$

$$dN_n^{(2)}/dt = k_pN_{n-1}^{(2)}M - k_pN_n^{(2)}M - (k_i' + k_i'')N_n^{(2)}M \quad (5)$$

$$dN_2^{(1,2)}/dt = 2k_i'N_1^{(1)}M + k_i'N_1^{(2)}M - 2k_pN_2^{(1,2)}M - k_i'N_2^{(1,2)}M \quad (6)$$

$$dN_n^{(1,2)}/dt = 2k_pN_{n-1}^{(1,2)}M + 2k_i'N_{n-1}^{(1)}M + k_i'N_{n-1}^{(2)}M - 2k_pN_n^{(1,2)}M - k_i'N_n^{(1,2)}M \quad (7)$$

$$dN_2^{(2,2)}/dt = k_i'N_1^{(2)}M - 2k_pN_2^{(2,2)}M - k_i'N_2^{(2,2)}M \quad (8)$$

$$dN_n^{(2,2)}/dt = 2k_pN_{n-1}^{(2,2)}M + k_i'N_{n-1}^{(2)}M - 2k_pN_n^{(2,2)}M - k_i'N_n^{(2,2)}M \quad (9)$$

$$dN_3^{(1,2,2)}/dt = k_i'N_2^{(1,2)}M + k_i'N_2^{(2,2)}M - 3k_pN_3^{(1,2,2)}M \quad (10)$$

$$dN_n^{(1,2,2)}/dt = 3k_pN_{n-1}^{(1,2,2)}M + k_i'N_{n-1}^{(1,2)}M + k_i'N_{n-1}^{(2,2)}M - 3k_pN_n^{(1,2,2)}M \quad (11)$$

The initial conditions of eqs 1–11 are

$$I|_{t=0} = I_0$$

$$M|_{t=0} = M_0$$

and

$$N_n^{(1)}|_{t=0} = N_n^{(2)}|_{t=0} = N_n^{(1,2)}|_{t=0} = N_n^{(2,2)}|_{t=0} = N_n^{(1,2,2)}|_{t=0} = 0$$

In order to solve eqs 1–11, we introduce a variable transformation:

$$x = k_p \int_0^t M dt$$

Then eqs 1–11 can be transformed into a set of linear differential equations:

$$dI/dx = -(a_1 + 2a_2)I \quad (12)$$

$$dN_1^{(1)}/dx = a_1I - (1 + 2a_2)N_1^{(1)} \quad (13)$$

$$dN_n^{(1)}/dx = N_{n-1}^{(1)} - (1 + 2a_2)N_n^{(1)} \quad (14)$$

$$dN_1^{(2)}/dx = 2a_2I - (1 + a_1 + a_2)N_1^{(2)} \quad (15)$$

$$dN_n^{(2)}/dx = N_{n-1}^{(2)} - (1 + a_1 + a_2)N_n^{(2)} \quad (16)$$

$$dN_2^{(1,2)}/dx = 2a_2N_1^{(1)} + a_1N_1^{(2)} - (2 + a_2)N_2^{(1,2)} \quad (17)$$

$$dN_n^{(1,2)}/dx = 2N_{n-1}^{(1,2)} + 2a_2N_{n-1}^{(1)} + a_1N_{n-1}^{(2)} - (2 + a_2)N_n^{(1,2)} \quad (18)$$

$$dN_2^{(2,2)}/dx = a_2N_1^{(2)} - (2 + a_1)N_2^{(2,2)} \quad (19)$$

$$dN_n^{(2,2)}/dx = 2N_{n-1}^{(2,2)} + a_2N_{n-1}^{(2)} - (2 + a_1)N_n^{(2,2)} \quad (20)$$

$$dN_3^{(1,2,2)}/dx = a_2N_2^{(1,2)} + a_1N_2^{(2,2)} - 3N_3^{(1,2,2)} \quad (21)$$

$$dN_n^{(1,2,2)}/dx = 3N_{n-1}^{(1,2,2)} + a_2N_{n-1}^{(1,2)} + a_1N_{n-1}^{(2,2)} - 3N_n^{(1,2,2)} \quad (22)$$

where $a_1 = k_i'/k_p$ and $a_2 = k_i''/k_p$. The initial conditions of the differential equations should be changed accordingly. Equations 12–22 are still too complicated to be solved by induction. Fortunately, the author of this work and co-workers have developed a graphical method^{2,5–7} by which we can easily find the rigorous solutions of some complex linear differential equations as given above.

Molecular Weight Distribution

In accordance with the definitions of Laplace transformation

$$F(\lambda) = \int_0^\infty e^{-\lambda x} f(x) dx \quad (23)$$

and

$$\lambda F(\lambda) - F(0) = \int_0^\infty e^{-\lambda x} \frac{df(x)}{dx} dx \quad (24)$$

Chart 1

[illegible]

Equations 12–22 can be transformed into a set of algebraic equations (see Chart 1):

$$(\lambda + a_1 + 2a_2)J/I_0 = 1 \quad (25)$$

$$(\lambda + 1 + 2a_2)M_1^{(1)} - a_1 J = 0 \quad (26)$$

$$(\lambda + 1 + 2a_2)M_n^{(1)} - M_{n-1}^{(1)} = 0 \quad (27)$$

$$(\lambda + 1 + a_1 + a_2)M_1^{(2)} - 2a_2J = 0 \quad (28)$$

$$(\lambda + 1 + a_1 + a_2)M_n^{(2)} - M_{n-1}^{(2)} = 0 \quad (29)$$

$$(\lambda + 2 + a_2)M_2^{(1,2)} - 2a_2M_1^{(1)} - a_1M_1^{(2)} = 0 \quad (30)$$

$$(\lambda + 2 + a_2)M_n^{(1,2)} - 2M_{n-1}^{(1,2)} - 2a_2M_{n-1}^{(1)} - a_1M_{n-1}^{(2)} = 0 \quad (31)$$

$$(\lambda + 2 + a_1)M_2^{(2,2)} - a_2M_1^{(2)} = 0 \quad (32)$$

$$(\lambda + 2 + a_1)M_n^{(2,2)} - 2M_{n-1}^{(2,2)} - a_2M_{n-1}^{(2)} = 0 \quad (33)$$

$$(\lambda + 3)M_3^{(1,2,2)} - a_2 M_2^{(1,2)} - a_1 M_2^{(2,2)} = 0 \quad (34)$$

$$(\lambda + 3)M_n^{(1,2,2)} - 3M_{n-1}^{(1,2,2)} - a_2M_{n-1}^{(1,2)} - a_1M_{n-1}^{(2,2)} = 0 \quad (35)$$

where J , $M_n^{(1)}$, $M_n^{(2)}$, $M_n^{(1,2)}$, $M_n^{(2,2)}$, and $M_n^{(1,2,2)}$ are the image functions of I , $N_n^{(1)}$, $N_n^{(2)}$, $N_n^{(1,2)}$, $N_n^{(2,2)}$, and $N_n^{(1,2,2)}$,

respectively. We can find the solutions of eqs 25–35 by way of the graphical method^{2,5–7}

$$J = \frac{I_0}{\lambda + a_1 + 2a_2} \quad (36)$$

$$M_n^{(1)} = \frac{I_0 a_1}{(\lambda + a_1 + 2a_2)(\lambda + 1 + 2a_2)^n} \quad (37)$$

$$M_n^{(2)} = \frac{I_0 2a_2}{(\lambda + a_1 + 2a_2)(\lambda + 1 + a_1 + a_2)^n} \quad (38)$$

$$M_n^{(1,2)} = \frac{I_0 2a_1 a_2}{\lambda + a_1 + 2a_2} \left\{ \frac{1}{\lambda + 3a_2} \left[\left(\frac{2}{\lambda + 2 + a_2} \right)^{n-1} - \left(\frac{1}{\lambda + 1 + 2a_2} \right)^{n-1} \right] + \frac{1}{\lambda + 2a_1 + a_2} \left[\left(\frac{2}{\lambda + 2 + a_2} \right)^{n-1} - \left(\frac{1}{\lambda + 1 + a_1 + a_2} \right)^{n-1} \right] \right\} \quad (39)$$

$$M_n^{(2,2)} = \frac{I_0 2 a_2^2}{(\lambda + a_1 + 2 a_2)^2} \left\{ \left(\frac{2}{\lambda + 2 + a_1} \right)^{n-1} - \left(\frac{1}{\lambda + 1 + a_1 + a_2} \right)^{n-1} \right\} \quad (40)$$

$$M_n^{(1,2,2)} = \frac{I_0 2a_1 a_2^2}{\lambda + a_1 + 2a_2} \left\{ \frac{1}{(\lambda + 3a_2)^2} \left[\frac{1}{2} \left(\frac{1}{\lambda + 1 + 2a_2} \right)^{n-2} - 2 \left(\frac{2}{\lambda + 2 + a_2} \right)^{n-2} + \frac{3}{2} \left(\frac{3}{\lambda + 3} \right)^{n-2} \right] + \frac{1}{\lambda + 2a_1 + a_2} \times \left[\frac{1}{\lambda + a_1 + 2a_2} \left(\frac{1}{\lambda + 1 + a_1 + a_2} \right)^{n-2} - \frac{2}{\lambda + 3a_2} \times \left(\frac{2}{\lambda + 2 + a_2} \right)^{n-2} \right] - \frac{1}{\lambda + 3a_1} \left[\frac{2}{\lambda + a_1 + 2a_2} \times \left(\frac{2}{\lambda + 2 + a_2} \right)^{n-2} - \frac{3}{\lambda + 3a_2} \left(\frac{3}{\lambda + 3} \right)^{n-2} \right] \right\} \quad (41)$$

An example of the derivation process of eqs 36–41 is given in Appendix 1. After the inversive Laplace

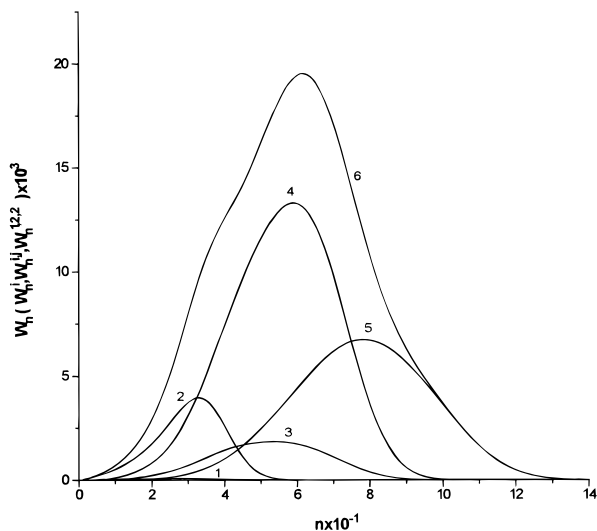


Figure 1. Molecular weight distribution curves of various species and the total resultant polymer, $I_0/M_0 = 0.001$, $a_1 = 0.01$, $a_2 = 0.05$, and $Y = 0.05$. (1) $W_n^{(1)}$; (2) $W_n^{(2)}$; (3) $W_n^{(1,2)}$; (4) $W_n^{(2,2)}$; (5) $W_n^{(1,2,2)}$.

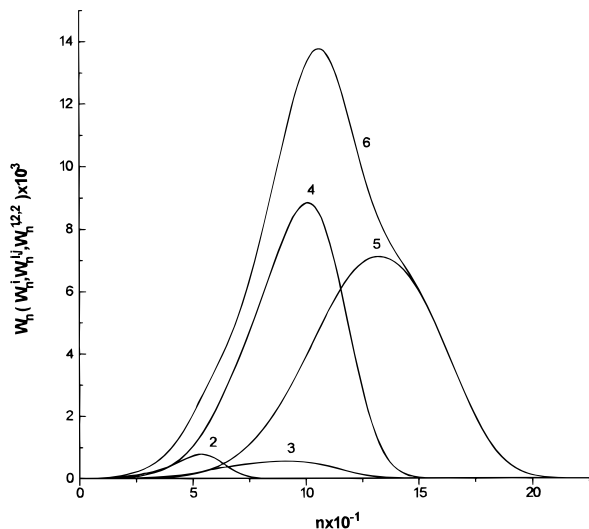


Figure 2. Molecular weight distribution curves of various species and the total resultant polymer, $Y = 0.1$. Other conditions are identical with those in Figure 1.

transformation of eqs 36–41, we obtain

$$I = I_0 e^{-(a_1 + 2a_2)x} \quad (42)$$

$$N_n^{(1)} = \frac{I_0 a_1}{(1 - a_1)^n} \left\{ e^{-(a_1 + 2a_2)x} - e^{-(1 + 2a_2)x} \sum_{i=0}^{n-1} \frac{[(1 - a_1)x]^i}{i!} \right\} \quad (43)$$

$$N_n^{(2)} = \frac{I_0 2a_2}{(1 - a_2)^n} \left\{ e^{-(a_1 + 2a_2)x} - e^{-(1 + a_1 + a_2)x} \sum_{i=0}^{n-1} \frac{[(1 - a_2)x]^i}{i!} \right\} \quad (44)$$

$$N_n^{(1,2)} = I_0 2a_1 a_2 \left\{ \frac{1}{(a_2 - a_1)(1 - a_1)^{n-1}} \times \left[e^{-x} \sum_{i=0}^{n-2} \frac{[(1 - a_1)x]^i}{i!} (e^{-(a_1 + a_2)x} + e^{-2a_2x}) - e^{-2x} \sum_{i=0}^{n-2} \frac{[2(1 - a_1)x]^i}{i!} e^{-a_2x} - e^{-(a_1 + 2a_2)x} \right] + \frac{1}{(a_1 - a_2)(1 - a_2)^{n-1}} \left[e^{-x} \sum_{i=0}^{n-2} \frac{[(1 - a_2)x]^i}{i!} (e^{-(a_1 + a_2)x} + e^{-2a_2x}) - e^{-2x} \sum_{i=0}^{n-2} \frac{[2(1 - a_2)x]^i}{i!} e^{-a_2x} - e^{-(a_1 + 2a_2)x} \right] \right\} \quad (45)$$

$$N_n^{(2,2)} = \frac{I_0 a_2^2 e^{-(a_1 + 2a_2)x}}{(1 - a_2)^n} \left\{ (n - 1) + \sum_{i=0}^{n-1} (n - 1 - i) \times \frac{[2(1 - a_2)x]^i e^{-2(1 - a_2)x}}{i!} - 2 \sum_{i=0}^{n-2} (n - 1 - i) \times \frac{[(1 - a_2)x]^i e^{-(1 - a_2)x}}{i!} \right\} \quad (46)$$

$$N_n^{(1,2,2)} = \frac{I_0 a_1 a_2^2}{(a_2 - a_1)^2 (1 - a_1)^{n-2}} \left\{ e^{-(a_1 + 2a_2)x} - e^{-(1 + a_2)x} \times \sum_{i=0}^{n-3} \frac{[(1 - a_1)x]^i}{i!} (e^{-a_2x} + 2e^{-a_1x}) + e^{-2x} \sum_{i=0}^{n-3} \frac{[2(1 - a_1)x]^i}{i!} \times (e^{-a_1x} + 2e^{-a_2x}) - e^{-3x} \sum_{i=0}^{n-3} \frac{[3(1 - a_1)x]^i}{i!} \right\} - \frac{I_0 a_1 a_2^2}{(a_1 - a_2)^2 (1 - a_2)^{n-2}} \left\{ e^{-(2a_2 + a_1)x} - e^{-(1 + a_2)x} \times \sum_{i=0}^{n-3} \frac{[(1 - a_2)x]^i}{i!} (e^{-a_2x} + 2e^{-a_1x}) + e^{-2x} \sum_{i=0}^{n-3} \frac{[2(1 - a_2)x]^i}{i!} \times (e^{-a_1x} + 2e^{-a_2x}) - e^{-3x} \sum_{i=0}^{n-3} \frac{[3(1 - a_2)x]^i}{i!} \right\} - \frac{I_0 a_1 a_2^2}{(a_1 - a_2)(1 - a_2)^{n-1}} \left\{ (n - 2) e^{-(2a_2 + a_1)x} - e^{-(1 + a_2)x} \times \sum_{i=0}^{n-3} (n - 2 - i) \frac{[(1 - a_2)x]^i}{i!} (e^{-a_2x} + 2e^{-a_1x}) + e^{-2x} \sum_{i=0}^{n-3} (n - 2 - i) \frac{[2(1 - a_2)x]^i}{i!} (e^{-a_1x} + 2e^{-a_2x}) - e^{-3x} \sum_{i=0}^{n-3} (n - 2 - i) \frac{[3(1 - a_2)x]^i}{i!} \right\} \quad (47)$$

An example of the inversive Laplace transformation is

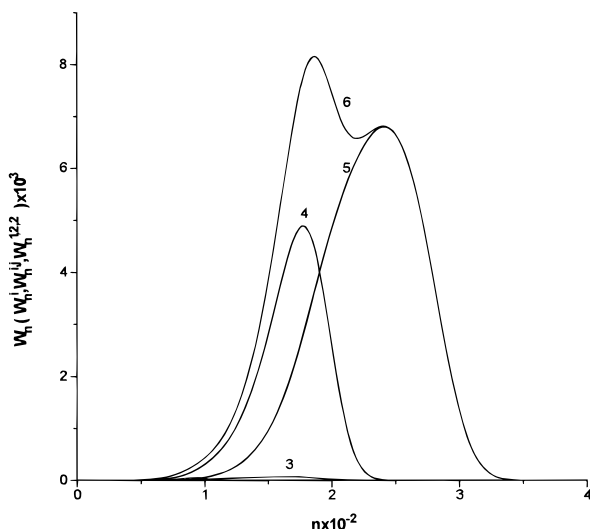


Figure 3. Molecular weight distribution curves of various species and the total resultant polymer, $Y = 0.2$. Other conditions are identical with those in Figure 1.

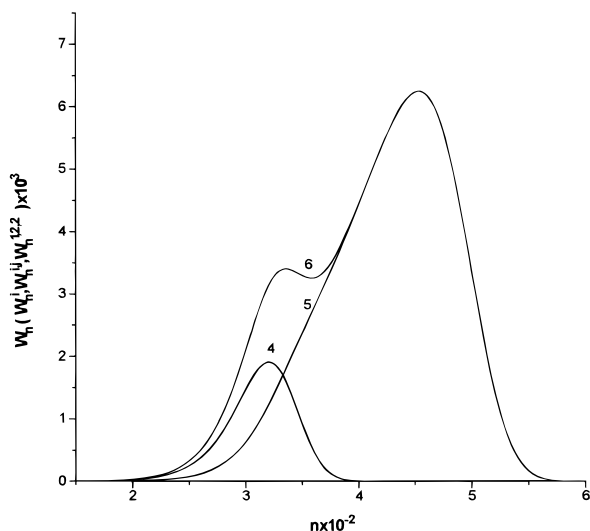


Figure 4. Molecular weight distribution curves of various species and the total resultant polymer, $Y = 0.4$. Other conditions are identical with those in Figure 1.

indicated in Appendix 2. Equations 43–47 are the molecular size distribution functions of the respective species. The molecular size distribution function of the total resulting polymer is

$$N_n = N_n^{(1)} + N_n^{(2)} + N_n^{(1,2)} + N_n^{(2,2)} + N_n^{(1,2,2)} \quad (48)$$

Even though the expressions of molecular size distribution of various species and total resulting polymer are rather complex, it is easy to carry out the numerical calculation by the aid of a personal computer.

Branching Distribution and Average Molecular Weight

In the polymerization system, there are various species with different numbers of arms. Provided B_1 , B_2 , and B_3 represent respectively the concentrations of the one-arm, the two-arm, and the three-arm species,

they can be defined as

$$B_1 = \sum_n (N_n^{(1)} + N_n^{(2)}) / \sum_n N_n \quad (49a)$$

$$B_2 = \sum_n (N_n^{(1,2)} + N_n^{(2,2)}) / \sum_n N_n \quad (49b)$$

$$B_3 = \sum_n N_n^{(1,2,2)} / \sum_n N_n \quad (49c)$$

Equation 49 are the so-called branching distributions of the resulting polymer. From eqs 26–35, we can get the concentrations of various species by means of inversive Laplace transformation:

$$\sum_n N_n^{(1)} = I_0 e^{-2a_2x} (1 - e^{-a_1x}) \quad (50)$$

$$\sum_n N_n^{(2)} = I_0 2e^{-(a_1+a_2)x} (1 - e^{-a_2x}) \quad (51)$$

$$\sum_n N_n^{(1,2)} = I_0 2\{e^{-a_2x} - e^{-2a_2x} + e^{-(a_1+2a_2)x} - e^{-(a_1+a_2)x}\} \quad (52)$$

$$\sum_n N_n^{(2,2)} = I_0 \{e^{-a_1x} + e^{-(a_1+2a_2)x} - 2e^{-(a_1+a_2)x}\} \quad (53)$$

$$\sum_n N_n^{(1,2,2)} = I_0 \{1 + e^{-2a_2x} - e^{-a_1x} - 2e^{-a_2x} + 2e^{-(a_1+a_2)x} - e^{-(a_1+2a_2)x}\} \quad (54)$$

$$\sum_n N_n = I_0 \{1 - e^{-(a_1+2a_2)x}\} \quad (55)$$

Hence

$$B_1 = \frac{e^{-2a_2x}(1 - e^{-a_1x}) + 2e^{-(a_1+a_2)x}(1 - e^{-a_2x})}{1 - e^{-(a_1+2a_2)x}} \quad (56)$$

$$B_2 = \frac{e^{-a_1x} + 2e^{-a_2x} - 2e^{-2a_2x} + 3e^{-(a_1+2a_2)x} - 4e^{-(a_1+a_2)x}}{1 - e^{-(a_1+2a_2)x}} \quad (57)$$

$$B_3 = \frac{1 - e^{-a_1x} + e^{-2a_2x} - 2e^{-a_2x} + 2e^{-(a_1+a_2)x} - e^{-(a_1+2a_2)x}}{1 - e^{-(a_1+2a_2)x}} \quad (58)$$

By a similar approach, the number- and the weight-average degrees of polymerization of the total resultant

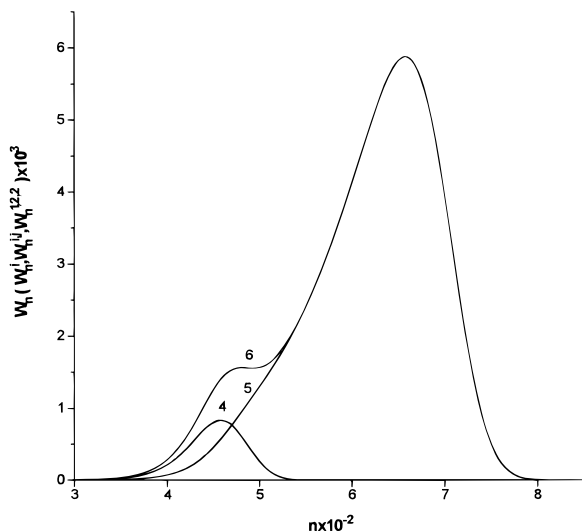


Figure 5. Molecular weight distribution curves of various species and the total resultant polymer, $Y = 0.6$. Other conditions are identical with those in Figure 1.

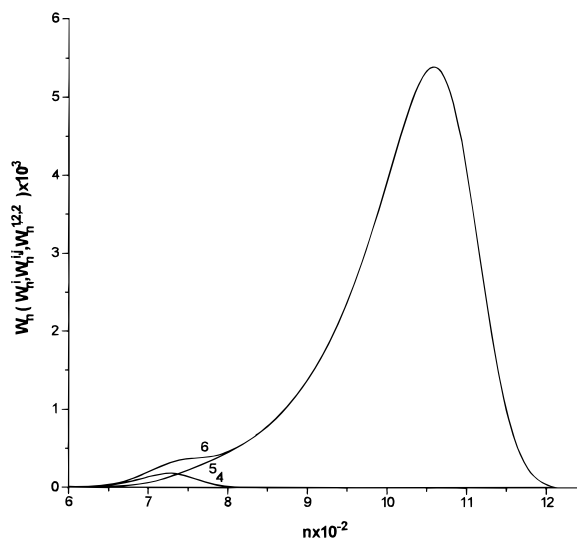


Figure 6. Molecular weight distribution curves of various species and the total resultant polymer, $Y = 1.0$. Other conditions are identical with those in Figure 1.

polymer can be derived:

$$\overline{P}_n = \frac{3x + \left(1 - \frac{1}{a_1}\right)(1 - e^{-a_1x}) + 2\left(1 - \frac{1}{a_2}\right)(1 - e^{-a_2x})}{1 - e^{-(a_1+2a_2)x}} \quad (59)$$

$$\begin{aligned} \overline{P}_w = & \left\{ 9x^2 + x\left(9 - \frac{2}{a_1} - \frac{4}{a_2}\right) - 2\left(1 - \frac{1}{a_2}\right)^2(1 - e^{-2a_2x}) - 4\left(1 - \frac{1}{a_1}\right)\left(1 - \frac{1}{a_2}\right)[1 - e^{-(a_1+a_2)x}] + \right. \\ & \left. \left(4x + 5 - \frac{2}{a_1} - \frac{4}{a_2}\right)\left[\left(1 - \frac{1}{a_1}\right)(1 - e^{-a_1x}) + 2\left(1 - \frac{1}{a_2}\right)(1 - e^{-a_2x})\right] \right\} / \left[3x + \left(1 - \frac{1}{a_1}\right)(1 - e^{-a_1x}) + 2\left(1 - \frac{1}{a_2}\right)(1 - e^{-a_2x}) \right] \quad (60) \end{aligned}$$

In all equations given above, there is only one variable,

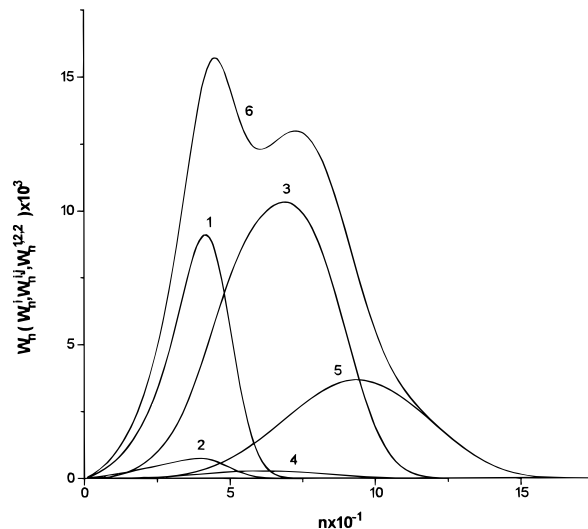


Figure 7. Molecular weight distribution curves of various species and the total resultant polymer: $I_0/M_0 = 0.001$, $a_1 = 0.05$, $a_2 = 0.01$, and $Y = 0.05$. (1) $W_n^{(1)}$; (2) $W_n^{(2)}$; (3) $W_n^{(1,2)}$; (4) $W_n^{(2,2)}$; (5) $W_n^{(1,2,2)}$.

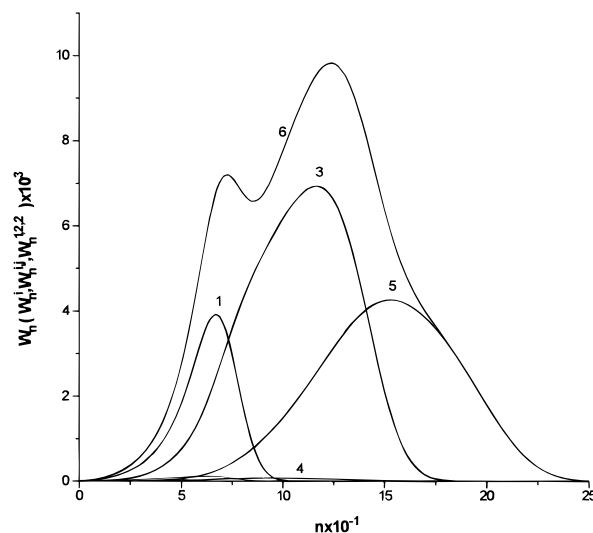


Figure 8. Molecular weight distribution curves of various species and the total resultant polymer, $Y = 0.1$. Other conditions are identical with those in Figure 7.

namely x , which can be determined by

$$Y = \frac{I_0}{M_0} \left\{ 3x + \left(1 - \frac{1}{a_1}\right)(1 - e^{-a_1x}) + 2\left(1 - \frac{1}{a_2}\right)(1 - e^{-a_2x}) \right\} \quad (61)$$

where Y is the monomer conversion. In terms of eq 61, we can estimate the value of variable x from monomer conversion and the initial reaction conditions. Then we can predicate the variation of various molecular parameters of the resulting polymer during the polymerization process.

Numerical Results and Discussion

The normalized molecular weight distribution functions for the various species and total polymer formed in the polymerization system are respectively defined

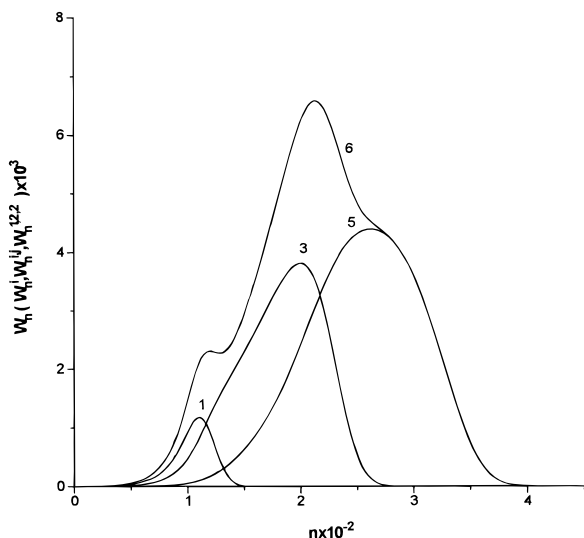


Figure 9. Molecular weight distribution curves of various species and the total resultant polymer, $Y = 0.2$. Other conditions are identical with those in Figure 7.

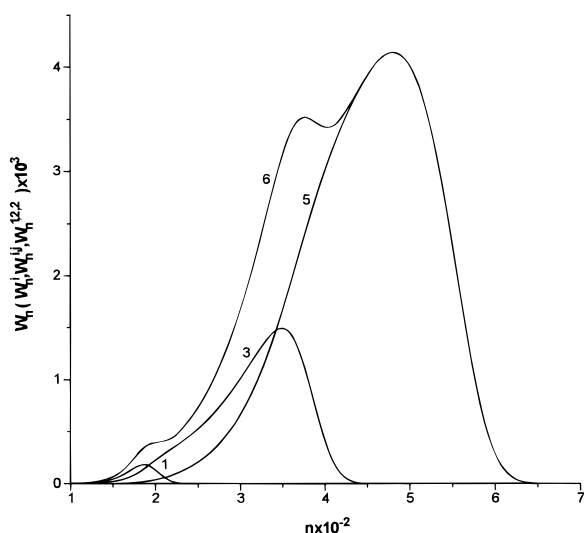


Figure 10. Molecular weight distribution curves of various species and the total resultant polymer, $Y = 0.4$. Other conditions are identical with those in Figure 7.

by

$$W_n^{(1)} = nN_n^{(1)} / \sum_n nN_n \quad (62)$$

$$W_n^{(2)} = nN_n^{(2)} / \sum_n nN_n \quad (63)$$

$$W_n^{(1,2)} = nN_n^{(1,2)} / \sum_n nN_n \quad (64)$$

$$W_n^{(2,2)} = nN_n^{(2,2)} / \sum_n nN_n \quad (65)$$

$$W_n^{(1,2,2)} = nN_n^{(1,2,2)} / \sum_n nN_n \quad (66)$$

$$W_n = nN_n / \sum_n nN_n \quad (67)$$

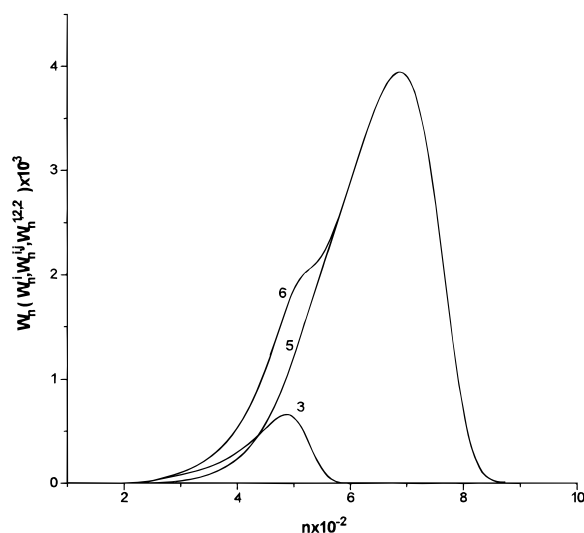


Figure 11. Molecular weight distribution curves of various species and the total resultant polymer, $Y = 0.6$. Other conditions are identical with those in Figure 7.

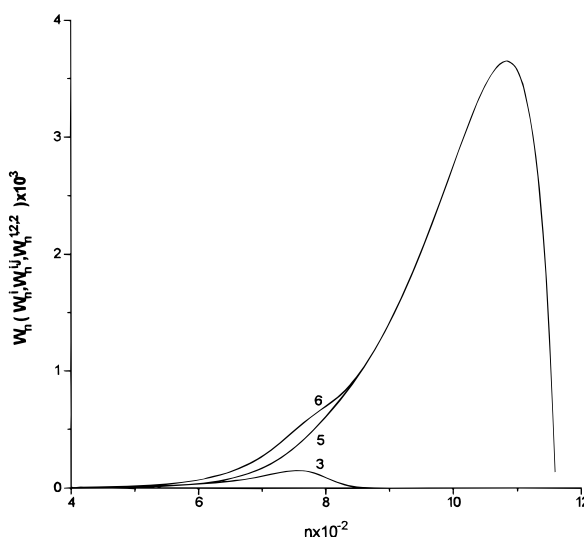


Figure 12. Molecular weight distribution curves of various species and the total resultant polymer, $Y = 1.0$. Other conditions are identical with those in Figure 7.

If there is only one functional group with lower initiation activity than the others in the trifunctional initiator, the changing of the molecular weight distribution curves of the various species and the total polymer with the monomer conversion are given in Figures 1–6. Alternatively, when the initiation rate constant of one functional group in the initiator is larger than that of other two active groups, the evolution of the molecular weight distribution curves of various species and the total products are indicated in Figures 7–12. Comparing the two sets of molecular weight distribution curves given with each other, we find that the effect of nonequal initiation rate constant on the molecular weight distribution curves is obvious at lower monomer conversion; however, the influence vanishes with the increasing of monomer conversion. The plots of the pertinent branching distribution versus monomer conversion are shown in Figures 13 and 14, respectively. Comparing Figure 13 with 14, we can conclude again that the influence of nonequal initiation rate constants on the molecular parameters of the resulting polymer

Chart 2

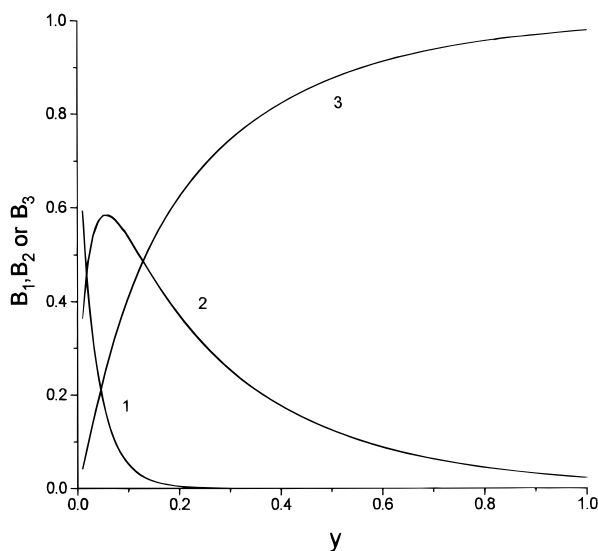
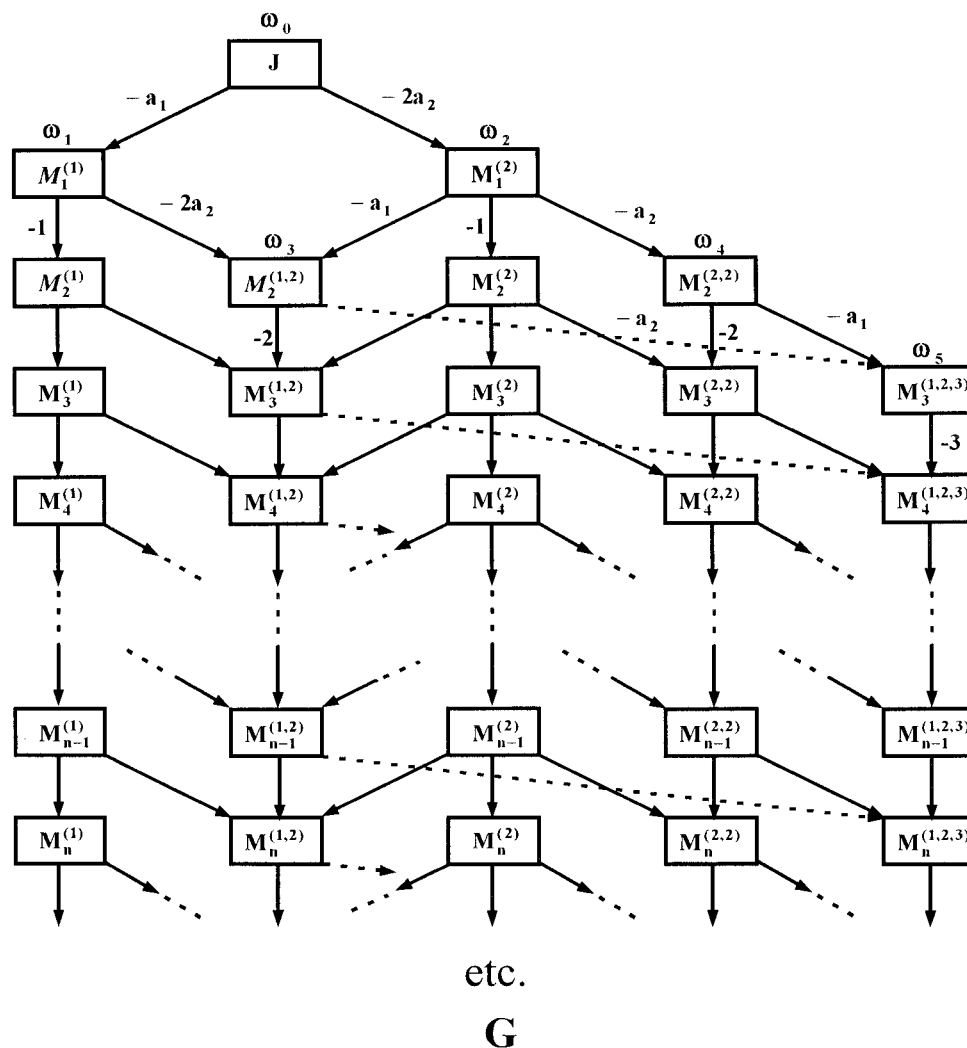


Figure 13. Branching distribution varying with monomer conversion, $a_1 = 0.01$, $a_2 = 0.05$, and $I_0/M_0 = 0.001$. (1) B_1 ; (2) B_2 ; (3) B_3 .

is rather important at low monomer conversion but becomes negligible at high polymer yield.

In this work we developed a kinetic model for the perfect living polymerization initiated by a trifunctional initiator taking account of nonequal initiation reactivi-

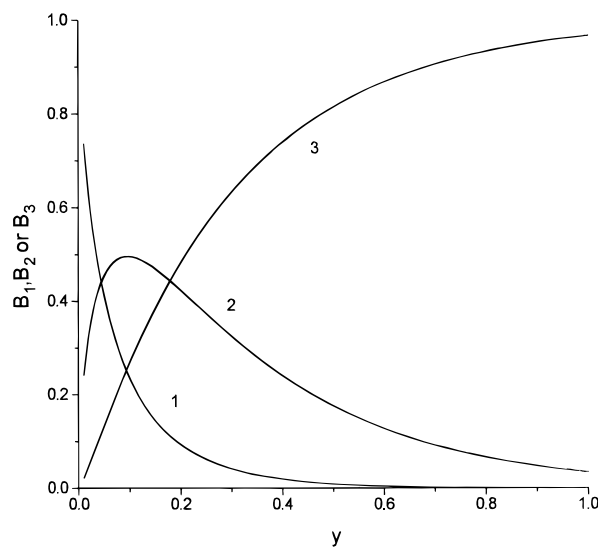
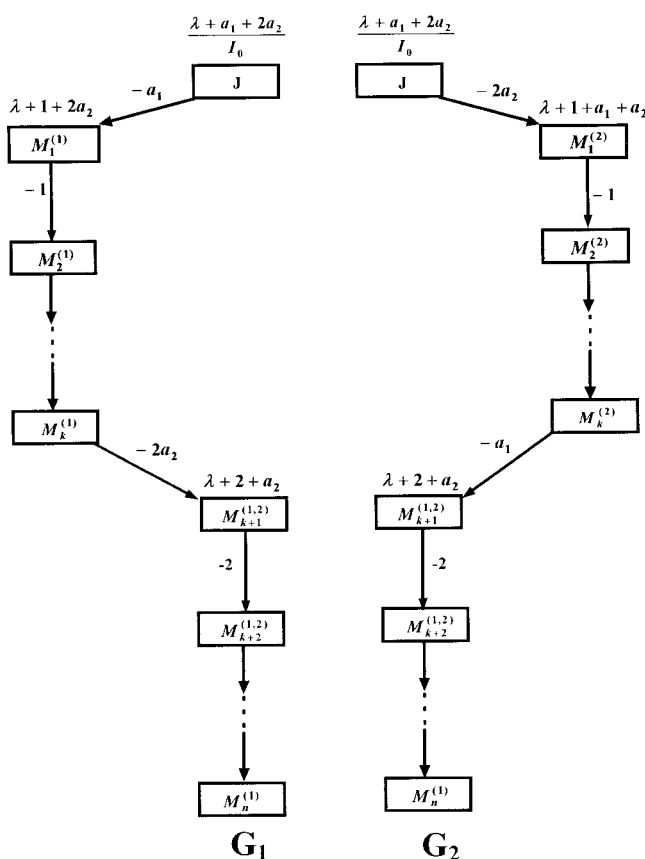


Figure 14. Branching distribution varying with monomer conversion, $a_1 = 0.05$, $a_2 = 0.01$, and $I_0/M_0 = 0.001$. (1) B_1 ; (2) B_2 ; (3) B_3 .

ties. Practically, most living polymerization systems are imperfect ones. There is an equilibrium between active and dormant species in both anionic and cationic living polymerization systems. The dormant effect of species may lead to a broadening of the molecular weight

Chart 3



distribution of the resulting polymer, especially at lower monomer conversion. The broadening of molecular weight distribution induced by the dormancy of species can be reduced somewhat in a star-branched polymer because a short arm within the star-shaped macromolecule can be compensated by a long arm. As a statistical result, the molecular weight distribution of star-branched polymers is usually narrower than that of linear ones.

Acknowledgment. This work was sponsored by National Natural Sciences Foundation of China.

Appendix 1

Equations 25–35 can be expressed as eq A1 (i.e., Chart 1), where

$$\begin{aligned}
 \omega_0 &= (\lambda + 2 + a_2)/I_0 \\
 \omega_1 &= \lambda + 1 + 2a_2 \\
 \omega_2 &= \lambda + 1 + a_1 + a_2 \\
 \omega_3 &= \lambda + 2 + a_2 \\
 \omega_4 &= \lambda + 2 + a_1 \\
 \omega_5 &= \lambda + 3
 \end{aligned} \quad (\text{A7})$$

The topology of the triangle coefficient matrix of eq A1 is related to graph G (Chart 2) in which each vertex corresponds to a diagonal element of the coefficient matrix, and every edge from a vertex to the next one is connected with a nondiagonal element of the same matrix. The weight of a vertex in graph G is equal to the pertinent diagonal element in the coefficient matrix,

and the weight of an edge in graph G is identical with the corresponding nondiagonal element in the coefficient matrix. The vertices of a certain column of graph G have the same weight; similarly, the edges connecting the vertices of a certain column or the edges between two neighboring columns also have the same weight. Therefore, in graph G we only marked the weights of the first vertex and the first edge in every column, and the weights of the edges between the top vertices of two neighboring columns. According to the graphical theorem, a root of eq A1, for instance $M_n^{(1,2)}$, is determined by the paths starting from vertex J to vertex $M_n^{(1,2)}$. Each of the paths contributes a term to the root, which can be expressed by a fraction with the factor $(-1)^n$, where n is the number of the edges in the path. The numerator of the fraction is the serial product of the all edge weights in the path, and the denominator of the fraction is a serial product of the all vertex weights in the path. There are two sorts of paths from J to $M_n^{(1,2)}$, which are shown in paths G₁ and G₂ (Chart 3). At first, we take account of path G₁. In terms of the graphical theorem mentioned above, the contribution of the path to root $M_n^{(1,2)}$ reads

$$\frac{I_0 2a_1 a_2}{2(\lambda + a_1 + 2a_2)} \left(\frac{1}{\lambda + 1 + 2a_2} \right)^k \left(\frac{2}{\lambda + 2 + a_2} \right)^{n-k}$$

In graph G₁, k runs from 1 to $n - 1$, so the total contributions of the all paths represented by G₁ are

$$\frac{I_0 2a_1 a_2}{2(\lambda + a_1 + 2a_2)} \sum_{k=1}^{n-1} \left(\frac{1}{\lambda + 1 + 2a_2} \right)^k \left(\frac{2}{\lambda + 2 + a_2} \right)^{n-k}$$

Similarly, the total contributions of the paths of G₂ type to root $M_n^{(1,2)}$ are

$$\frac{I_0 2a_1 a_2}{2(\lambda + a_1 + 2a_2)} \sum_{k=1}^{n-1} \left(\frac{1}{\lambda + 1 + a_1 + a_2} \right)^k \left(\frac{2}{\lambda + 2 + a_2} \right)^{n-k}$$

Therefore, we have

$$M_n^{(1,2)} = \frac{I_0 2a_1 a_2}{2(\lambda + a_1 + 2a_2)} \sum_{k=1}^{n-1} \left\{ \left(\frac{1}{\lambda + 1 + 2a_2} \right)^k + \left(\frac{1}{\lambda + 1 + a_1 + a_2} \right)^k \right\} \left(\frac{2}{\lambda + 2 + a_2} \right)^{n-k} \quad (\text{A2})$$

From eq A2, we can easily get eq 40. $M_n^{(1)}$, $M_n^{(2)}$, $M_n^{(2,2)}$, and $M_n^{(1,2,2)}$ were derived by a similar way.

Appendix 2

In accordance with the Reimann–Mellin theorem, the inversive Laplace transformation of $M_n^{(1,2)}$, for instance, can be performed:

$$N_n^{(1,2)} = \frac{1}{2\pi i} \int_{-i\infty}^{+i\infty} M_n^{(1,2)} e^{\lambda x} d\lambda = \sum_j \text{res}(M_n^{(1,2)} e^{\lambda x})_{\lambda=\lambda_j} \quad (\text{A3})$$

where the integral is defined along the imaginary axis in the complex plane, λ_j is a pole of function $(M_n^{(1,2)} e^{\lambda x})$ located in the left side of the imaginary axis, and res is the symbol of residuum. In function $(M_n^{(1,2)} e^{\lambda x})$, there are three first-order poles, i.e., $\lambda_0 = -(a_1 + 2a_2)$, $\lambda_1 =$

$-3a_2$, and $\lambda_2 = -(2a_1 + a_2)$, and three $(n-1)$ th-order poles, i.e., $\lambda_3 = -(2 + a_2)$, $\lambda_4 = -(1 + a_1 + a_2)$, and $\lambda_5 = -(1 + 2a_2)$. The corresponding residua of the first-order poles are

$$\text{res}(M_n^{(1,2)} e^{\lambda x})_{\lambda_0} = I_0 2a_1 a_2 e^{-(a_1+2a_2)x} \times \left\{ \frac{1}{a_2 - a_1} \left[\left(\frac{2}{2 - a_1 - a_2} \right)^{n-1} - \left(\frac{1}{1 - a_1} \right)^{n-1} \right] + \frac{1}{a_1 - a_2} \left[\left(\frac{2}{2 - a_1 - a_2} \right)^{n-1} - \left(\frac{1}{1 - a_2} \right)^{n-1} \right] \right\} \quad (\text{A4})$$

$$\text{res}(M_n^{(1,2)} e^{\lambda x})_{\lambda_1} = 0 \quad (\text{A5})$$

$$\text{res}(M_n^{(1,2)} e^{\lambda x})_{\lambda_2} = 0 \quad (\text{A6})$$

The respective pertinent residua of the $(n-1)$ th-order poles are

$$\text{res}(M_n^{(1,2)} e^{\lambda x})_{\lambda_3} = \frac{I_0 2^n a_1 a_2}{(n-2)!} \left\{ \frac{e^{\lambda x}}{d\lambda^{n-2} \lambda + a_1 + 2a_2} \times \left[\frac{1}{\lambda + 3a_2} + \frac{1}{\lambda + 2a_1 + a_2} \right] \right\}_{\lambda_3} = -I_0 2a_1 a_2 e^{-(2+a_2)x} \times \sum_{i=0}^{n-2} \frac{(2x)^i}{i!} \left\{ \frac{1}{(a_1 - a_2)(1 - a_2)^{n-1}} \left(\frac{1}{1 - a_2} \right)^i + \frac{1}{(a_2 - a_1)(1 - a_1)^{n-1}} \left(\frac{1}{1 - a_1} \right)^i \right\} \quad (\text{A7})$$

$$\text{res}(M_n^{(1,2)} e^{\lambda x})_{\lambda_4} = \frac{I_0 2a_1 a_2}{a_1 - a_2} e^{-(1+a_1+a_2)x} \times \sum_{i=0}^{n-2} \frac{x^i}{i!} \left\{ \frac{(1 - a_2)^i}{(1 - a_2)^{n-1}} - \frac{(1 - a_1)^i}{(1 - a_1)^{n-1}} \right\} \quad (\text{A8})$$

$$\text{res}(M_n^{(1,2)} e^{\lambda x})_{\lambda_5} = \frac{I_0 2a_1 a_2}{a_2 - a_1} e^{-(1+2a_2)x} \times \sum_{i=0}^{n-2} \frac{x^i}{i!} \left\{ \frac{1}{(1 - a_1)^{n-1-i}} - \frac{1}{(1 - a_2)^{n-1-i}} \right\} \quad (\text{A9})$$

Substituting eqs A4–A9 into eq A3, we obtain eq 45.

References and Notes

- (1) Fijumoto, T. *Macromolecules* **1978**, *11*, 673.
- (2) Rein, D.; Rempp, P.; Lutz, P. *J. Makromol. Chem., Macromol. Symp.* **1993**, *67*, 237.
- (3) Yan, D.; Li, G.; Jiang, Y. *Sci. Sin.* **1981**, *24*, 46.
- (4) Yan, D. In *Polymeric Materials Encyclopedia*; Salamone, J. C., Ed.; CRC Press: Inc.: Boca Raton, FL, 1996; Vol. 6, p 4481.
- (5) Karspa, M.; Trekoval, J. Czechoslovakia Patent CS 203,519, 1983; *Chem. Abstr.* **1983**, *99*, 176043Z. Karspa, M.; Trekoval, J. Czechoslovakia Patent CS 209,263, 1983; *Chem. Abstr.* **1983**, *99*, 213074H.
- (6) Shulga, R. P.; Lebedev, V. S. *Vysokomolek. Soed.* **1978**, *A20*, 1345.
- (7) Yan, D. *J. Chem. Phys.* **1984**, *80*, 3434.
- (8) Yan, D. *J. Macromol. Sci.-Chem.* **1986**, *A23*, 129.
- (9) Yan, D. *Macromolecules* **1988**, *22*, 2926.

MA971113E